Engineered Science
DOI: https://dx.doi.org/10.30919/es965

Synthesis and Characterization of Salt Tolerant Ternary Polyampholyte as Rheology Enhancer and Fluid Loss Additive for Water-Based Drilling Fluids

Nurbatyr Mukhametgazy,[1, 2,*] Iskander Sh.Gussenov,[1, 2] Alexey V. Shakhvorostov,[1] Heikki Tenhu,[3] Munziya Abutalip[4] and Sarkyt E. Kudaibergenov[1,*]

Abstract

A novel ternary polyampholyte (TPA) was synthesized via free radical copolymerization in deionized water using ammonium persulfate as an initiator. The TPA composition included 80 mol.% acrylamide (AAm), 10 mol.% 2-acrylamido-2-methyl-1-propanesulfonic acid sodium salt (AMPS), and 10 mol.% (3-acrylamidopropyl) tri-methylammonium chloride (APTAC). TPA was used as an alternative to low viscosity polyanionic cellulose (PAC-LV) to prepare bentonite-based drilling fluids with different concentrations of NaCl (1-35 wt.%). Gel strength (GS) measurements demonstrated that, at a 6:1 [initiator]:[catalyst] ratio, even in high salinity brines (25-35 wt.%), the GS values exceeded industry standards, highlighting the superior performance of bentonite/ternary polyampholyte (BT/TPA) in high salinity media. Notably, TPA addition significantly reduced the filter cake thickness to 0.09 cm, outperforming BT/PAC-LV (0.18 cm) and bentonite alone (0.41 cm). Furthermore, the BT/TPA drilling fluid exhibited the lowest permeability/thickness ratio at 13 mD/cm, indicating its potential as a rheology enhancer and fluid loss additive for salt-resistant Water-Based Drilling Fluids (WBDF) applications. The filtration performance of bentonite and bentonite/polymer dispersions showed a clear trend in fluid loss values: BT/TPA < BT/PAC-LV < Base Fluid. The high-salinity BT/TPA drilling fluid had remarkably low fluid loss, measuring just 3.5 ml, well below the API standard limit of 12 ml.

Keywords: Ternary polyampholyte (TPA); Low viscosity polyanionic cellulose PAC-LV; Bentonite clay (BT); High salinity media; Rheology enhancer; Gel strength; Filter cake; Fluid loss additive; Salt-resistant Water-Based Drilling Fluids (WBDF).
Received: 18 July 2023; Revised: 15 September 2023; Accepted: 16 September 2023.
Article type: Research article.

1. Introduction

Oil-, synthetic-, and water-based drilling fluids are usually used in drilling operations.[1-3] Oil-based and synthetic drilling fluids are rarely used due to the high cost and environmental issues.[4,5] Water-based drilling fluids (WBDF) are widely used because they are less environmentally hazardous, easy to handle, relatively low-cost, and effective.[5-7] In fact, rheology and fluid-loss are among the most important properties of drilling fluids.[8]

In order to modify the rheological properties of WBDF bentonite is usually used. Good rheological properties of bentonite and its ability to form a thin and low-permeability filter cake make it suitable for drilling operations.[8] Hydration, swelling, and flocculation of bentonite particles in drilling conditions, negatively affects rheological properties of WBDF and their ability to form a thin and low-permeability filter cake.[9-11] Temperature and salinity are the most important factors, which affect the stability of bentonite particles in WBDF.[12] Of note is that 4.0 and 8.0 wt.% pure bentonite suspensions showed non-Newtonian behavior.[13] Remarkably, in some studies rheological properties of polymer solutions were compared to those of BT/polymer dispersions in

[1] *Institute of Polymer Materials and Technology, Almaty 050019, Kazakhstan.*
[2] *Department of Chemical and Biochemical Engineering, Satbayev University, Almaty 050013, Kazakhstan.*
[3] *Department of Chemistry, University of Helsinki, Helsinki, Finland.*
[4] *Lab of Renewable Energy, National Laboratory Astana, Nazarbayev University, Astana, 010000, Kazakhstan.*
**Email:* Nurbatyr.kaz@gmail.com (N. Mukhametgazy), skudai@mail.ru (S. E. Kudaibergenov)

deionized water at low and relatively high temperatures.[14] However, in real conditions deionized water is never available that is why there is a need to study the properties of BT/polymer based fluids in low and high salinity brines.

Different polymeric additives can be used in combination with bentonite in order to improve the performance of WBDF.[15] For example, a number of studies aimed the improvement of the rheology,[16,18-22] as well as fluid-loss properties[20,23,24] of WBDF. In fact, natural polymers (cellulose, starch, xanthan gum, and guar gum) and modified natural polymers (for example, polyanionic cellulose (PAC), carboxymethyl cellulose (CMC), nanocellulose, and nanostarch) have been used in combination with bentonite to improve the properties of WBDF. The wide use of these materials is supported by their eco-friendliness and low-cost.[25-28] However, natural polymers and their modified forms are intolerant to microbial degradation and are unstable at higher than 115 °C.[26]

Amphoteric polymers can make WBDF more tolerant to high salinity at elevated temperatures.[29,30] In this regard, polyampholytes are of great interest, because of their ability to increase viscosity with the increase in salinity.[31,32] Additionally, amphoteric polymers are believed to electrostatically attract negatively charged bentonite layers, which results in the reduction of fluid loss.[33] Moreover, amphoteric polymers promote the shear-thinning behavior of fluids - high viscosity at low shear rates, to suspend and carry cuttings, and low viscosity at a high shear rates for fast rotation of drilling instruments at high pressure.[34] Recently.[35,36] temperature and salt-resistant polyampholyte gels were used as fluid loss additive and plugging agent for WBDF.

In this work, a new ternary polyampholyte AAm-*co*-AMPS-*co*-APTAC was synthesized, characterized, and evaluated as potential additives for WBDF in a wide range of salinity (1-35 wt.% NaCl). The novel TPA was designed to improve the salt tolerance and overall performance of drilling fluids.

2. Experimental

2.1 Materials

The monomers including: acrylamide (AAm, 97% purity), 2-acrylamido-2-methylpropanesulfonic acid sodium salt (AMPS, 50 wt.%), (3-acrylamidopropyl) trimethylammonium chloride (APTAC, 75 wt.% in water), and ammonium persulfate, $(NH_4)_2S_2O_8$ (APS, 98% purity), N, N, N', N'-tetramethylethylenediamine (TMEDA) were purchased from Sigma-Aldrich (USA). (PAC-LV, 97% purity) "Shandong Look Chemical co., Ltd" (Shandong province, China). Nitrogen (purity 99.995 wt.%) "Ikhsan TechnoGas" Ltd. (Almaty, Kazakhstan), acetone (purity 99.9 wt.%) "Labchimprom" Ltd. (Almaty, Kazakhstan) were used without further purification. Sodium chloride, NaCl (99% purity wt.%) was purchased from "Titan Biotech LTD" (Rajasthan, India), which was used in mass concentration range from 1 to 35 wt.%. Bentonite clay was supplied by BENTO LUX LLC, Tatarstan, Russia, in accordance with the American Petroleum Institute (API) standard. It is widely used for drilling wells in the oilfields of Kazakhstan.

The average particle size of pure bentonite, determined through zeta-potential measurements using a Zetasizer NanoZS 90 (Malvern, UK), was found to be 5.34-7.18 μm. The bentonite used for studying the rheology and fluid loss properties of WBDF was applied without further purification The chemical composition of the bentonite sample was analyzed using an X-ray fluorescence spectrometer (XRF) with the RFA analyzer Epsilon (Netherlands), 2015 (see Fig. 1). The composition of the bentonite clay, given in weight percent (wt.%), is as follows: MgO-0.92; Al_2O_3-6.886; SiO_2-25.463; P_3O_4-0.459; $FeCl_2$-0.196; K_2O-3.278; CaO-1.566; TiO_2-0.705; V_2O_5-0.018; Cr_2O_3-0.016; MnO_2-0.052; Fe_2O_3-7.927; Ni_2O_3-0.007; CuO-0.005; ZnO-0.015; Ga_2O_3-0.004; Rb_2O-0.022; SrO-0.025; Y_2O_3-0.005; ZrO_2.

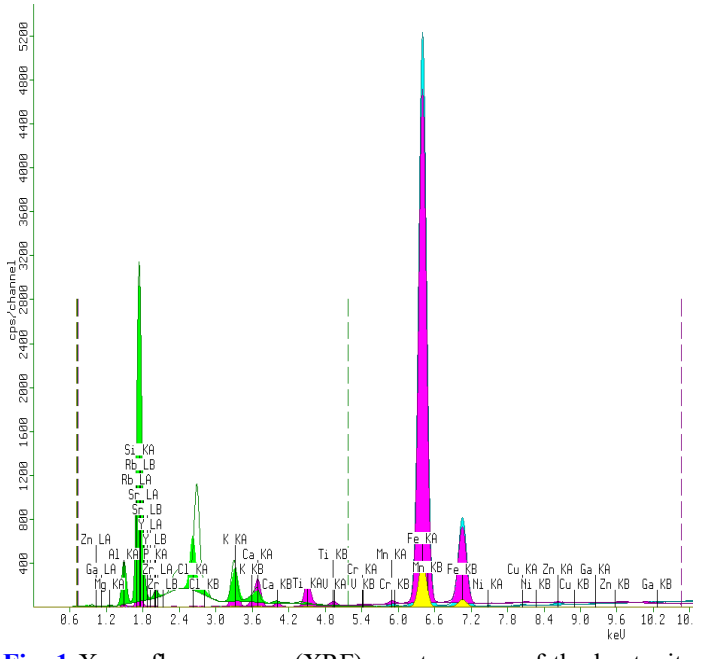

Fig. 1 X-ray fluorescence (XRF) spectroscopy of the bentonite clay.

Special hardened 6.3-cm diameter filter papers with a pore size of 25-30 μm, obtained from Fann Instrument Company in Houston, Texas, USA, were used in fluid loss tests according to the API standard. These tests involved different formulations of bentonite/polymer dispersions.

Table 1. Synthetic protocol of AAm-*co*-AMPS-*co*-APTAC in deionized water.

Initial feed composition, mol. %	Samples No. / Monomers	I	II	III	IV	V	VI	VII
80	AAm (g)	5.9						
10	AMPS (g)	4.84						
10	APTAC (g)	2.91						
[Initiator]:[Catalyst] [APS]/[TMEDA], mol/mol		6:1	8:1	6:1	4:3	12:1	18:1	12:1
H_2O (wt.%)		50	40	30	50	50	50	50
Yield mass of TPA (g)		15.8	20.9	14.7	14.3	-	18.2	18.3
Temperature (°C)		0±1	0±1	0±1	24±1	24±1	0±1	24±1
Apparent viscosity (mPa·s)		27.3	11.4	5.2	9.7	-	14.5	7.1

2.2 Methods

2.2.1 Synthesis of ternary polyampholyte AAm-*co*-AMPS-*co*-APTAC

The ternary polyampholyte (TPA) AAm-*co*-AMPS-*co*-APTAC was synthesized via-conventional free radical (co)polymerization of monomers according to synthetic protocol given in Table 1. The rheology of the TPA was studied within a wide range of NaCl content in brine.

Initially, the dry AAm monomer was dissolved in deionized water while being stirred in a beaker at relevant temperature. Then, the liquid monomers, AMPS and APTAC, were added in equimolar concentrations to the aqueous solution of AAm, total concentration of the monomers in water was kept constant (50 wt.%), however the amount of water was changed between 50 and 30 wt.%. The monomer mixture was purged with nitrogen over 1 h continually to remove the dissolved oxygen. Afterward, the mixture of 0.005-0.01 mol.% APS as initiator and 0.008-0.03 mol.% TMEDA as catalyst was added to speed up the radical polymerization. The polymerization process, accompanied by increasing of solution viscosity, occurred over 2 hrs.

In order to select appropriate samples with optimal viscosity, apparent viscosity measurements were conducted using an AMETEK Brookfield viscometer at a shear rate of 7.32 s^{-1} and room temperature. As a result, the 0.5 wt.% TPA-I in 23.2 wt.% NaCl brine was chosen due to its highest apparent viscosity among all the samples are presented in Table 1.

2.2.2 Spectroscopic methods

FTIR spectrum of AAm-*co*-AMPS-*co*-APTAC terpolymer was recorded on a Cary 660 FTIR (Agilent, USA).

^{1}H and ^{13}C-NMR spectra of the terpolymers dissolved in D_2O (10 mg/mL) were recorded at room temperature on a Avance-III 500 MHz (Bruker, Germany) using D_2O as a solvent at 20 °C. Chemical shifts were measured relative to signals of residual protons and carbons of the deuterated solvent.

Elemental analysis of TPA samples for C, H, N and S were performed using Vario EL-III elemental analyzer (Elementary Analyze System GmbH, Hanau, Germany).

2.2.3 Gel-permeable chromatography (GPC)

The average molecular weights (M_w and M_n) of aqueous solutions of AAm-*co*-AMPS-*co*-APTAC were measured by gel permeation chromatography (GPC) using a Viscotek (Malvern) chromatograph equipped with 270 dual detectors (Malvern) and VE 3580 RI detector (Malvern).

2.2.4 Thermogravimetric analysis (TGA)

TGA was carried out using LabSys Evo equipment (Setaram, France) at temperature range of 30 to 500 °C and heating rate of 10 °C/min.

2.2.5 TEM and SEM measurements

The SEM images were obtained on a Crossbeam 540 (Germany) by placing dry polymer powder coated with gold nanoparticles on carbon tape. The TEM images were made on a JEOL JEM 1400 Plus (U.S.A) by placing one drop of 0.01 wt.% polymer solution in D_2O on a copper cell (d=2 mm) and drying the sample overnight in a refrigerator.

2.2.6 Chemical analysis

The elemental composition of bentonite clay sample was determined by XRF using RFA analyzer Epsilon (Netherlands).

2.2.7 Zeta-potential

The zeta-potentials were measured using a Zetasizer NanoZS 90 (Malvern, UK), equipped with a 633 nm laser source.

2.2.8 Preparation of bentonite/water and bentonite/polymer dispersions

As a first step, 2 wt.% polymer solutions were prepared in 1-35 wt.% NaCl brines by using magnetic stirrer. The solutions

were stirred for 24 h at 1000 rpm and aged in static conditions for the next 24 h for complete hydration of polymers. As the second step, bentonite/polymer dispersions were prepared by slowly adding 4 wt.% of bentonite powder to the polymer solutions were being stirred. Each bentonite/polymer dispersion was poured in a covered container and static standing for 24 h for the complete swelling of the bentonite clay at room temperature.[15,35] As a result, several BT/TPA-I and BT/PAC-LV dispersions were prepared using brines with a wide range of NaCl concentrations. Moreover, bentonite dispersions (without polymer) were prepared in deionized water and 35 wt.% NaCl brine in order to compare their rheological and fluid loss properties with those of bentonite/polymer dispersions. In order to keep bentonite particles uniformly suspended in the drilling fluid before starting rheological experiments the samples were agitated for 1 h.

The measured pH of the bentonite/polymer dispersions was found to be 5.6 ± 0.04 that is unfavorable especially for stabilization of the BT/PAC-LV system. This is attributed to the negative charges of both bentonite particles (-16 mV, as per zeta-potential measurement) and PAC-LV, which is categorized as an anionic polyelectrolyte. However, in case of bentonite/TPA system due to the presence of 10 mol.% of positively charged monomer APTAC the bentonite-TPA mixture might have bigger stability. This positively charged APTAC component can contribute to the stabilization of the bentonite particles. In our case the pH value was measured only for the BT/TPA+35 wt.% drilling fluid.

2.2.9. Rheological study

The apparent and reduced viscosities of 2 wt.% TPA-I and PAC-LV solutions in various brine solutions were measured using an AMETEK Brookfield viscometer (Spindle - 0) at a shear rate of 7.32 s^{-1} and room temperature. The viscosity and shear stability of 4 wt.% bentonite with 2 wt.% polymer BT/TPA and BT/PAC-LV dispersions in 1-35 wt.% NaCl brine at 25±1°C were determined using an Anton Paar Rheolab QC rotational rheometer (Austria). The measurements were conducted with a temperature control device (C-LTD80/QC) and a cylindrical measuring system (CC39/QC-LTD). Shear stress (τ) and viscosity (η) were determined over a wide range of shear rates (γ= 1-1000 s^{-1}) at 25 °C. The rheological properties of the bentonite and bentonite/polymer formulations were analyzed using the Herschel-Bulkley model.[14]

$$\tau = \tau_o + K(\gamma)^n \quad (1)$$

where K (Pa·s^n), n and τ_o (Pa) are consistency coefficient, flow behavior index and yield stress, respectively.

GS was measured by using API standard procedure at a low shear rate of 5.1 s^{-1}.[14] Prior to the measuring of the 10 s GS, the samples were pre-sheared for 1 min at 510 s^{-1} and left undisturbed for 10 s. Then the sample was again left undisturbed for 10 min before measuring 10 min GS.

2.2.10 Fluid loss tests

Fluid loss tests were performed according to the API standard procedure for the evaluation of WBDFs.[37] The fluid loss volume of the BT/polymer dispersions was measured using a VM-6-type medium-pressure filtration apparatus through a filter paper (Fann, U.S.A.) with a pore size of 25-30 µm. In a single test, 120 mL of drilling fluid was forced to pass through the filter paper by applying a pressure of 0.7 MPa for 30 minutes.[38] The filtrate volume was recorded after each 5 min. After the filtration, the filter paper was carefully detached from the filter press cup in order to measure the thickness of the available cake on the paper.

2.2.11 Permeability of filter cake, and SEM analysis

For the measurement of permeability of filter cakes, Darcy's law was used, and SEM analysis was carried out for the study of filter cake morphology after drying overnight at 100 °C using JEOLJSM-6490 LA (JEOL Ltd, Japan).

3. Results and Discussion

The discussion section is divided into four sections. The first section focuses on the synthesis and characterization of the ternary polyampholyte. The second section presents the rheological properties of TPA and PAC-LV solutions without bentonite. The third section describes the rheological properties of bentonite/polymer dispersions. The fourth section discusses the results of fluid loss tests, including measuring the permeability of filter cakes, as well as SEM analysis of formulated filter cakes derived from bentonite/polymer dispersions following the filtration tests.

3.1 Synthesis and characterization of AAm-*co*-AMPS-*co*-APTAC terpolymer

The ternary polyampolytes (TPA) composed of AAm, AMPS and APTAC were synthesized by free radical polymerization in relevant amount of deionized water by using APS as initiator and TMEDA as catalyst under nitrogen atmosphere at 0 and 24±1 °C for 30 min. The resulting terpolymers belong to random polyampholytes, the repeating monomeric units consisting of 80 mol.% AAm, 10 mol.% AMPS, and 10 mol/% APTAC (see Fig. 2).

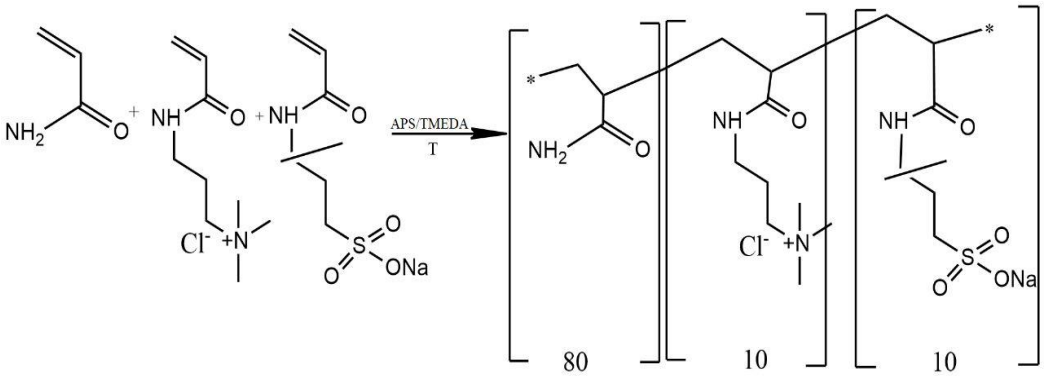

Fig. 2 Synthesis of AAm-*co*-AMPS-*co*-APTAC=80:10:10 terpolymer.

The FTIR spectrum of the amphoteric terpolymer is shown in Fig. 3(a). The wide absorption band in the region of 3200-3500 cm^{-1} corresponds to the NH_2 groups of AAm, and the absorption bands in the region of 2800-3000 cm^{-1} correspond to the asymmetric and symmetric vibrations of the CH groups. The absorption bands at 1660 and 1546 cm^{-1} belong to the vibrations of the N-substituted groups, Amide I and Amide II, respectively. The absorption band at 1450 cm^{-1} is characteristic of the deformation vibrations of the CH groups. Finally, the absorption band in the region of 1190 cm^{-1} is related to the symmetrical S=O stretching vibration of AMPS. Furthermore, the structure of the TPA was established by using ^{1}H and ^{13}C-NMR spectroscopy, which are shown in Figs. 3(b) and 3(c), respectively. Several characteristic peaks are observed in the spectra of TPA due to the presence of different monomers. In Fig. 3(b), the broad resonance peaks at 1.6-1.8 and 2.3 ppm are attributed to the protons of the methylene and methine groups of the polymer backbone, respectively. However, these peaks are overlapped with methyl and methylene protons of AMPS and APTAC. The peaks at 3.1-3.3 ppm were assigned to the shifted protons of the methyl and methylene groups of AMPS and APTAC. The appearance of the peak at 1.4 ppm can be attributed to two methylene groups of AMPS.

As seen from the ^{13}C-NMR spectra (Fig. 3(c)), the peak at 16.78 ppm is related to $-CH_2$ carbons (a), and the peak at around 23.72 ppm belongs to $-CH_3$ and $-CH-$ carbons (b, c) of APTAC or Na-AMPS backbone. The peak at 52.99 ppm corresponds to $-CH_2-SO_3-$ (d) in the Na-AMPS segment, while the peaks at 57.43 and 64.74 ppm belong to the –CN (e) in the APTAC segment. Additionally, the peak at 179.48 ppm is characteristic of C=O (g) groups in acrylamide units. Meanwhile, there was no peak in the region of 100−150 ppm, indicating the absence of any monomer.[17-19] Thus, the ^{1}H and ^{13}C-NMR spectra confirm the successful synthesis of the AAm-*co*-AMPS-*co*-APTAC=80; 10:10 ternary polyampholytes.

Elemental analysis (C, H, N, S) was conducted to determine the composition of TPA at high temperature, in the presence of oxygen and catalyst. The S and N elements were oxidized to SO_2 and N_2, respectively. The gases were separated in chromatographic column by the carrier gas. Finally, the different elements were detected in the thermal conductivity cell and analyzed. Based on the principles of mass conservation and the element conservation, the ratios of different monomers in the copolymer were calculated as shown in Fig. 3(d). The elemental analysis of the copolymer synthesized at molar ratio of monomers [AAm]:[AMPS]:[APTAC] = 80:10:10 mol.% indicates that the measured value of the element content in the copolymer was consistent with the theoretical value. This suggests that the resulting product was the intended target product.

The Fig. 3(e) shows the TGA curve of AAm-*co*-AMPS-*co*-APTAC terpolymer (black line), and differential thermogravimetric curve DTG (red line) registered in N_2 atmosphere. The mass loss of the copolymer can be divided into several stages that are shown by dotted lines. The fluctuated stages between 117 and 239 °C, where the mass loss is 12%, can probably be attributed to evaporation of moisture containing in sample. The second significant mass loss ranging from 239 to 343 °C and the peak occurred at 318 °C, with mass loss about 21%, probably corresponds to the decomposition of the amide group of the copolymer. The third stage between 343 and 487 °C, resulting in weight loss of 31%, with the peak at 402 °C, may be related to decomposition of sulfonic groups and C-C backbones of polymer chain. The latest stage between 402 and 500 °C can be the result of fully carbonization of polymer chain. It is concluded that the thermal stability of TPA is rather high and suitable for use as temperature resistant polymeric additive in WBDFs.

3.2. Determination of the molecular weights of AAm-*co*-APTAC-*co*-AMPS terpolymer

Table 2 and Fig. 4 represent the GPC data and molecular

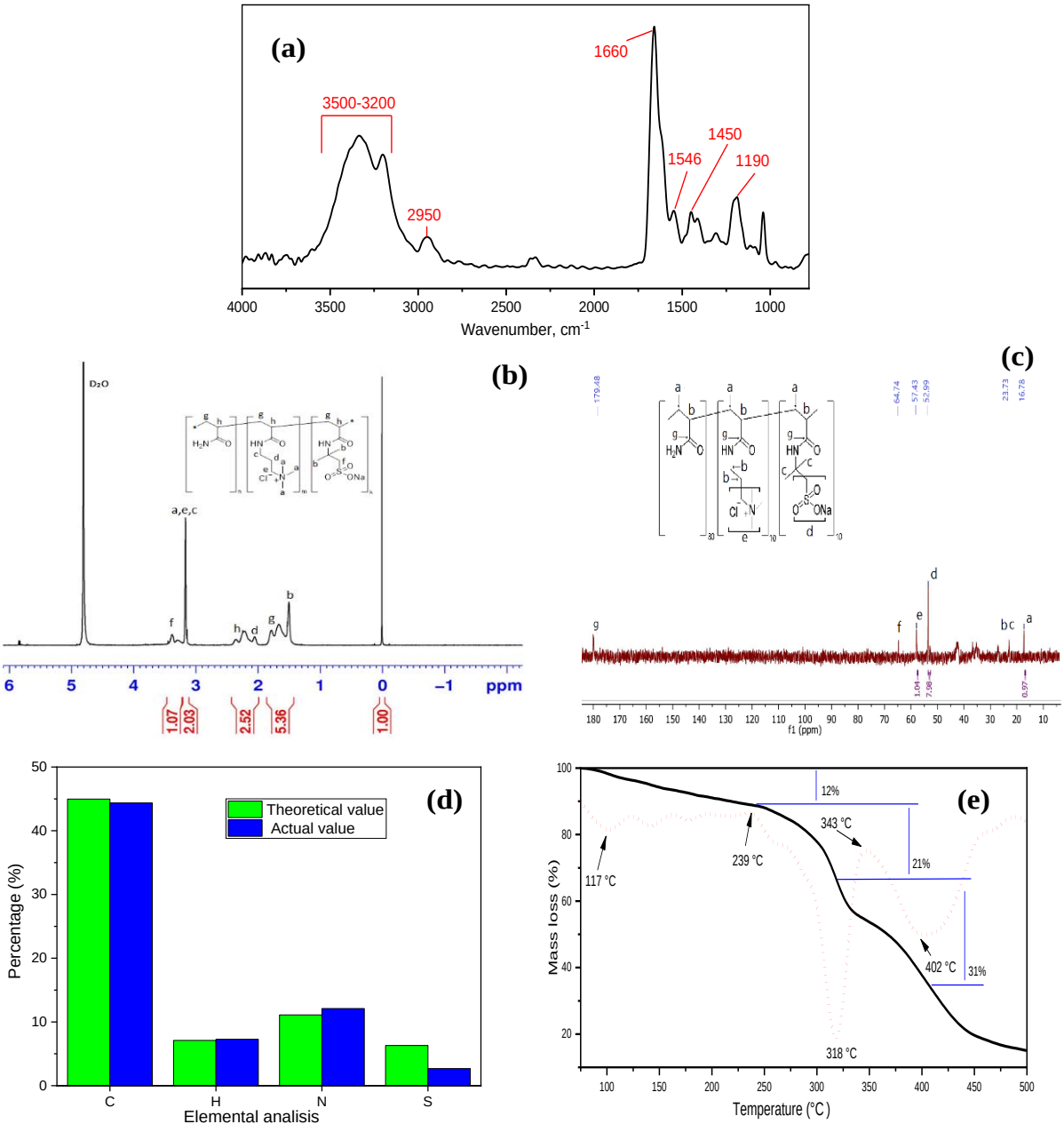

Fig. 3 Characterization of AAm-co-AMPS-co-APTAC terpolymer.

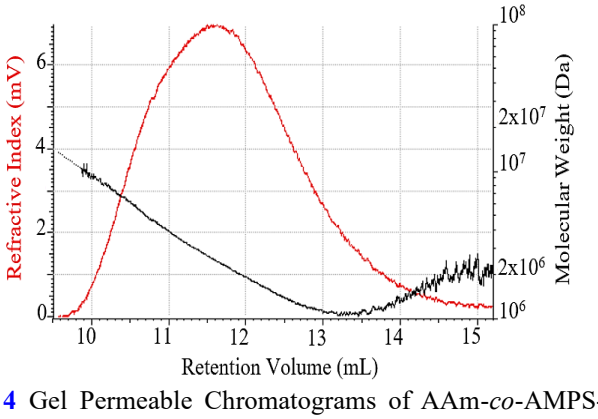

Fig. 4 Gel Permeable Chromatograms of AAm-*co*-AMPS-*co*-APTAC terpolymer in aqueous solution.

Table 2. M_w, M_n and PDI of AAm-*co*-APTAC-*co*-AMPS terpolymer.

Composition, mol. %			$M_w \cdot 10^6$, Dalton	$M_n \cdot 10^6$, Dalton	PDI = M_w/M_n
AAm	APTAC	AMPS			
80	10	10	2.9	2.1	1.36

weights of AAm-*co*-AMPS-*co*-APTAC terpolymer measured in aqueous solution. The weight-average molecular weight (M_w) and the average-number molecular weight (M_n) of the terpolymer was equal to 2.9×10^6 and 2.1×10^6 Dalton,

respectively. The polydispersity index (PDI) of the terpolymer is quite low for conventional free radical polymerization. The relatively high monomer concentration in the reaction mixture is considered to be responsible for the low PDI. The high molecular weight and low PDI of the terpolymer are expected to be suitable for oil recovery.

3.3 Zeta potential measurements

Zeta potential measurements were conducted using 0.1 wt.% bentonite and AAm-*co*-AMPS-*co*-APTAC terpolymer in deionized water. Fig. 5(a) and Fig. 5(b) show the zeta potential values of the pure bentonite dispersion and the aqueous solution of TPA-I, respectively. In the aqueous solution, the average hydrodynamic size and zeta potential of bentonite were determined to be 5.34 µm and ξ= -16 mV, respectively. On the other hand, the average hydrodynamic size and zeta potential of the TPA-I in the aqueous solution were found to be 5.8 nm and ξ= -2.57 mV, respectively. The small negative charge of TPA-I can be attributed to a small excess of AMPS-Na monomer in the polymer chain, indicating different reactivity among the monomers. The slightly negative surface charge (ξ= -2.57 mV) of the TPA is expected to facilitate the adsorption and intercalation of positively charged monomers on the edges of bentonite pellets, making it resistant to salt cations.

However, when 4% bentonite was added to a high salinity solution (35 wt.% NaCl) and stirred at 1000 rpm for 30 minutes, it formed a suspension. Subsequently, the suspension was left undisturbed for 24 hours to allow the bentonite particles to swell. Afterward, a portion of the bentonite particles separated from the suspension, with some settling and others remaining in suspension. The comparative filter cakes in deionized water and 35 wt.% brine after their API filtration test are shown in Fig. 6.

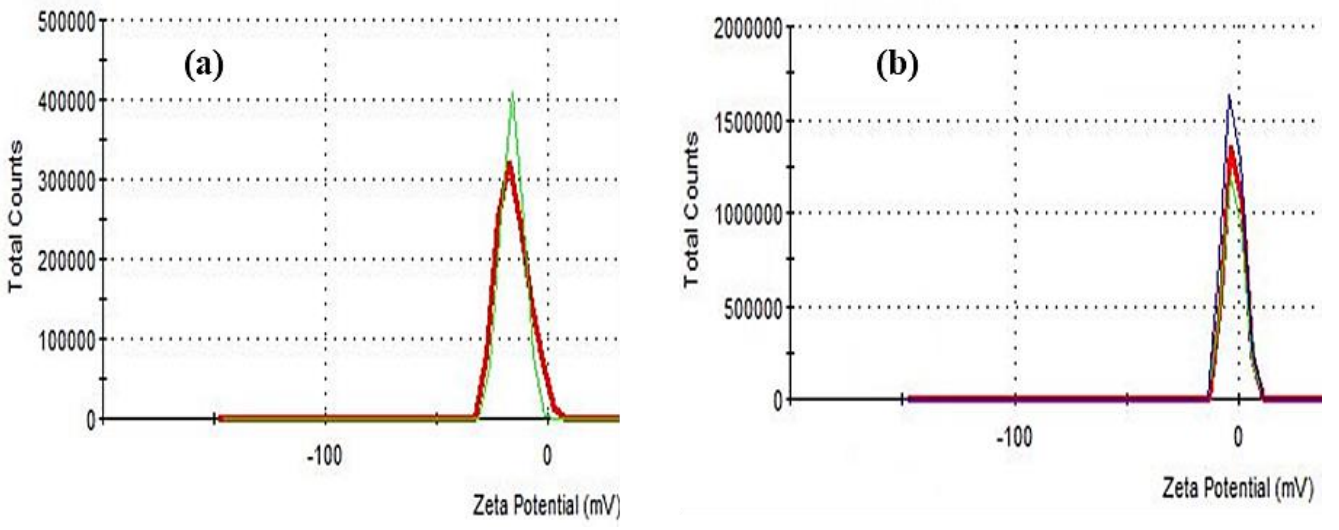

Fig. 5 Zeta potential values of 0.1 wt.% pure bentonite dispersion (a) and aqueous solution of TPA (b).

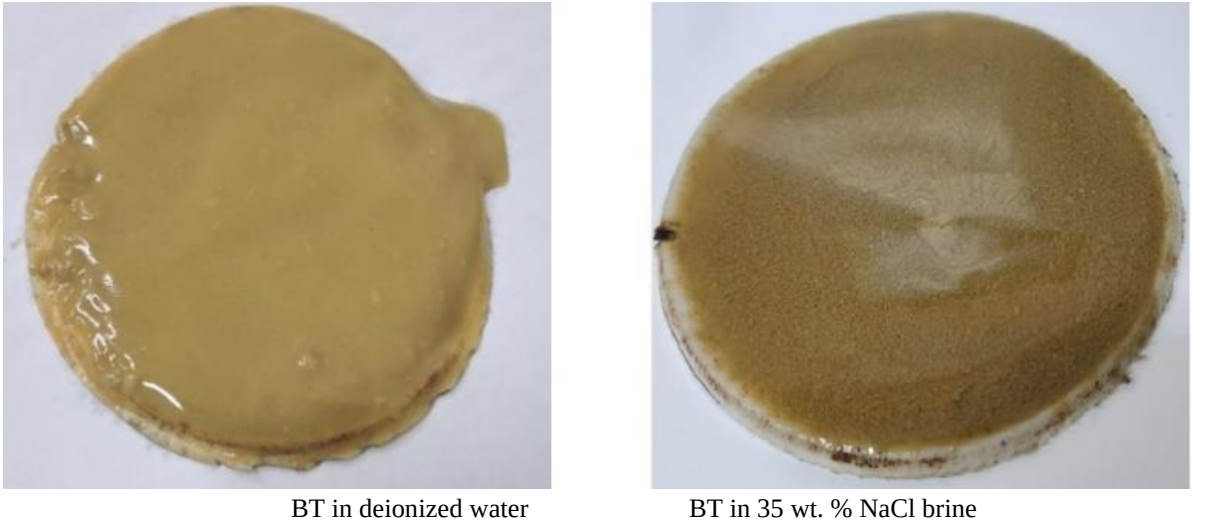

BT in deionized water BT in 35 wt. % NaCl brine

Fig. 6 The bentonite-based filter cakes formed in deionized water (left) and 35 wt. % NaCl brine (right).

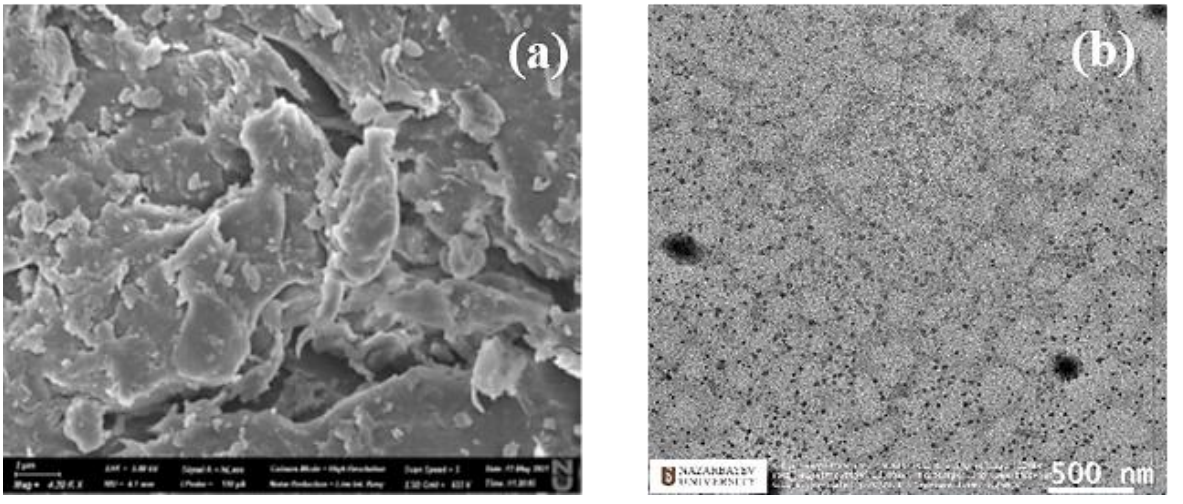

Fig. 7 SEM (a) and TEM (b) images of AAm-*co*-AMPS-*co*-APTAC terpolymer.

3.4 SEM and TEM results

Figure 7 shows the SEM (a) and TEM (b) images of AAm-*co*-AMPS-*co*-APTAC terpolymer in the form of powder and thin film, respectively. SEM photo shows the compact polymer microscopic structures with several hydrated shells and intermolecular connections looking like a fish-bone framework structure. In contrast, the TEM image of amphoteric terpolymer shows spherical nanoparticles and branched structure, with average sizes of 25-30 nm and 200-250 nm, respectively. Furthermore, the number of small nanoparticles is vastly larger than that of big ones.

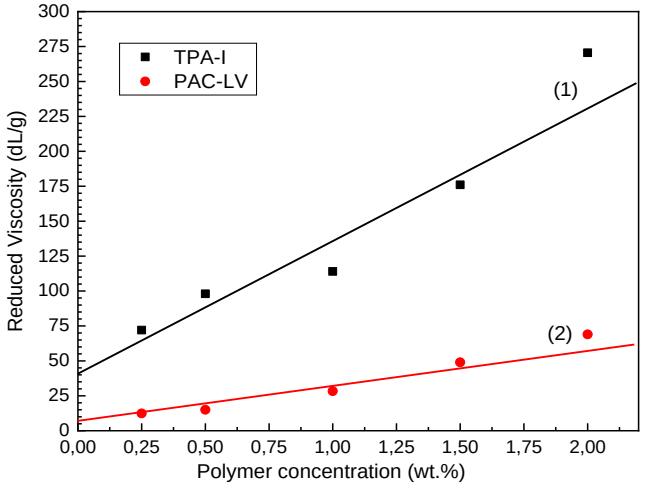

Fig. 8 Reduced viscosities of TPA-I (1) and PAC-LV (2) in a saline solution containing 35 wt.% NaCl at 24 ˚C.

3.5 Rheological study

3.5.1 The intrinsic viscosities [η] of polymer solutions

The intrinsic viscosities [η] of TPA-I and PAC-LV measured in 35 wt.% NaCl brine is shown in Fig. 8. The method of determination of the intrinsic viscosity of TPA-I can be found in Ref. [39]. The reduced viscosity η_{sp}/C of TPA-I and PAC-LV decreased from 270.5 to 75 dL·g^{-1} and from 69 to 12.4 dL·g^{-1}, respectively, in the concentration range of polymers from 2 to 0.25%. Extrapolation of η_{sp}/C to $C \rightarrow 0$ allows to determine the intrinsic viscosities of TPA-I and PAC-LV that are equal to 41 and 7.5 dL/g, respectively. The high value of the intrinsic viscosity of TPA-I in 35 wt.% NaCl salt solution confirms the high molecular weight of prepared polyampholyte.

3.5.2 The apparent viscosities of polymer solutions

Figure 9 shows a significant difference in the apparent viscosity and shear stress versus shear rate of the polymer solutions (without bentonite) in salinity of brine at 25 °C.

As shown in Fig. 9(a), at 1 % and 7 % NaCl salinity and a wide range of shear rates, the apparent viscosity of TPA-I polymer decreased from 0.38 to 0.04 Pa·s and 0.6 to 0.04 Pa·s, respectively. It is noteworthy that with the increase of the shear rate from 1 to 1000 s^{-1}, the viscosity values of TPA-I prepared in 1, 7, 15, 25 and 35 wt.% NaCl brines decrease from 0.38 to 0.035 Pa·s and from 1.14 to 0.09 Pa·s, respectively.

As can be seen from Fig. 9(b), the increase of NaCl concentration from 1 to 35 wt.% results in the increase of apparent viscosity of PAC-LV from 0.04 to 0.15 Pa·s (3.7 times increase) at a shear rate of 1 s^{-1}. However, at a high shear rate of 1000 s^{-1}, there is only 1.7 fold increase in viscosity (from 0.027 to 0.046 Pa·s) with the increase in salinity.

In 35 wt.% NaCl brine at a shear rate of 1 s^{-1}, there is a substantial difference in viscosity values between the polymer solutions, ranging from 1.14 to 0.15 Pa·s for TPA-I and PAC-LV, respectively. These results demonstrate that in high salinity conditions (35 wt.% NaCl) the viscosity values of TPA-I solutions are notably higher than those of PAC-LV at low and high shear rates.

The flow curves (shear stress versus shear rate) of TPA-I and PAC-LV polymer solutions are depicted in Figs. 9(c) and (d). At a constant shear rate of 5.1 s^{-1} (API standard procedure), the PAC-LV polymer solution exhibits lower shear stress compared to the TPA-I polymer solution. In fact, the YS values of TPA-I and PAC-LV polymer solutions in a 35 wt.% NaCl brine are equal to 2.99 Pa and 0.24 Pa, respectively. Across the entire range of shear rates (1-1000 s^{-1}), the shear stress values observed for TPA-I and PAC-LV polymer solutions,

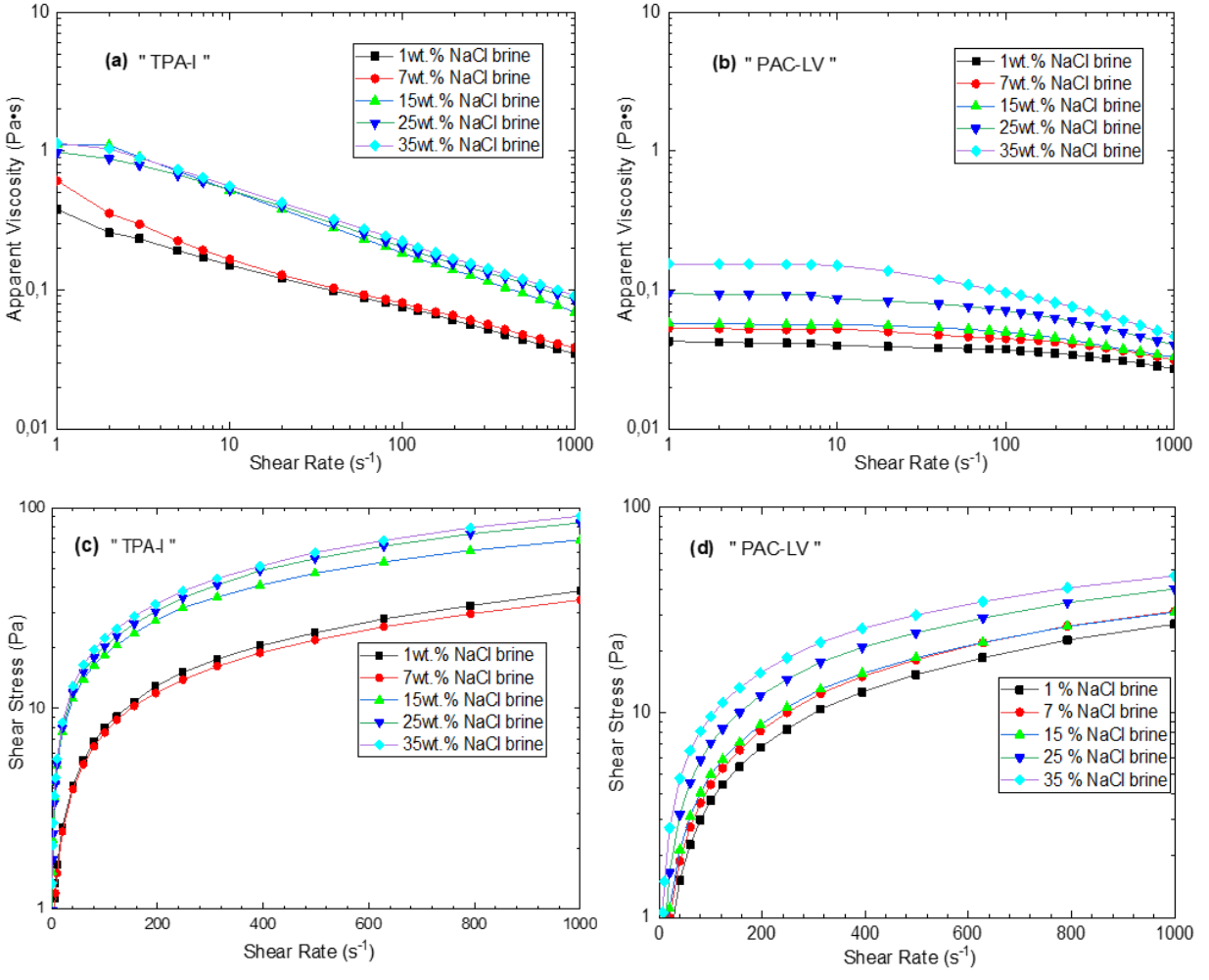

Fig. 9 Apparent viscosity (a, b) and shear stress (c, d) versus shear rate for 2 wt.% TPA-I and PAC-LV polymer solutions in concentration 1, 7, 15, 25 and 35 wt.% of NaCl brine at 25 °C.

prepared by using 1-15 wt.% NaCl brines, are lower than those observed for the same polymer solutions prepared by using 25-35 wt.% NaCl brines. Of note, TPA-I polymer solution prepared by using 35 wt.% NaCl brine exhibits the highest shear stress value among tested solutions.

As shown in Figs. 9(c) and (d), the shear stress values observed for TPA-I and PAC-LV polymer solutions in 35 wt.% NaCl saline water are ranging from 1.34 to 90.9 Pa and from 0.063 to 46.4 Pa, respectively. This indicates that the shear stress of TPA-I is sufficiently higher compared to PAC-LV. Therefore, it can be observed that polyampholyte terpolymers exhibit higher GS under similar temperature and shear rate conditions. For both polymer solutions the shear stress increases with salinity.

Figure 10 demonstrates the change of apparent viscosity of TPA-I and PAC-LV polymer solutions across a wide range of NaCl concentrations (1-35 wt.%). The TPA-I (1) curve shows that the lowest viscosity values (34.7 and 38.5 mPa·s) were observed when the concentration of NaCl was equal to 1 and 7 wt.% NaCl. The increase of salinity to 15 and 35 wt.% resulted in the viscosity increase up to 69.1 and 90.9 mPa·s, respectively.

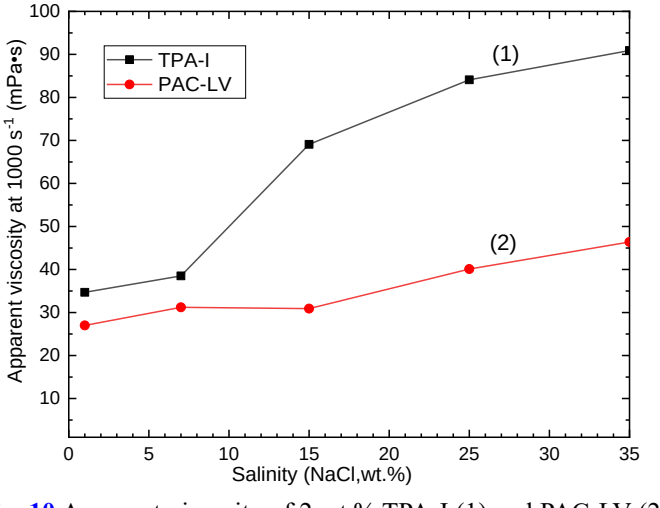

Fig. 10 Apparent viscosity of 2 wt.% TPA-I (1) and PAC-LV (2) polymer solutions versus NaCl concentration at 1000 s^{-1} and 25 °C.

Of note is that the viscosity increase of PAC-LV with salinity was less significant. In fact, the increase of salinity from 1 to 35 wt.% NaCl resulted in the increase of viscosity

from 27 to 46.4 mPa·s. This observation suggests that in high salinity and under high shear rate the PAC-LV solution is less effective than TPA-I terpolymer.

Based on the results obtained from rheology measurements of TPA-I solutions across a wide range of brine concentrations, selections were made for further testing with BT/TPA-I to create a salt-tolerant water-based drilling fluid formulations. Simultaneously, the properties of these formulations were compared with those of BT/PAC-LV with brine.

3.5.3 Rheological properties of Bentonite/Polymer dispersions

The rheological properties of BT/TPA-I or BT/PAC-LV dispersions were investigated at 25 °C across a wide range of shear rates and NaCl concentrations. Fig. 11(a) shows the steady shear viscosity of BT/TPA-I dispersion versus shear rate. The comparison of Fig. 9(a) and Fig. 11(a) with zoomed view show that the addition of bentonite to TPA-I solution increases the viscosity of the formulations in 35 wt.% NaCl brine at a shear rate of 1 s^{-1} from 1.14 to 3.83 Pa·s.

As observed in Fig. 11(b), the viscosity of BT/PAC-LV formulations in 35 wt.% NaCl brine exhibited significantly lower values across a wide range of shear rates, ranging from 0.26 to 0.05 Pa·s, compared to BT/TPA-I formulations, which ranged from 3.83 to 0.08 Pa·s. Additionally, upon comparing Fig. 9(b) and Fig. 11(b), it can be noted that the presence of bentonite did not have a substantial impact on the viscosity of PAC-LV, which measured 0.15 and 0.26 Pa·s, respectively, at a shear rate of 1 s^{-1} in 35 wt.% NaCl brine.

The flow curves of BT/TPA-I and BT/PAC-LV dispersions are shown in Figs. 12(a) and (b), respectively, at 25 °C. All the curves exhibit non-Newtonian shear thinning behavior. As can be seen, BT/TPA-I terpolymer dispersions demonstrate higher shear stress values compared to BT/PAC-LV dispersions. Of note is that the shear stress increases with salinity.

The rheological parameters obtained for bentonite/polymer dispersions using the Herschel-Bulkley model are presented in Table 3. Consistency coefficient 'K' shows the relation between the shear stress and shear rate, interactions between the components of the drilling fluid and its cleaning efficiency. The YS values at zero shear rate for the BT/TPA-I dispersions were found to be maximum at 5.29 Pa and 2.99 Pa in 25 and 35 wt.% NaCl brines, respectively (refer to Table 3). In contrast, the BT/PAC-LV dispersions exhibited significantly lower YS values (Table 3).

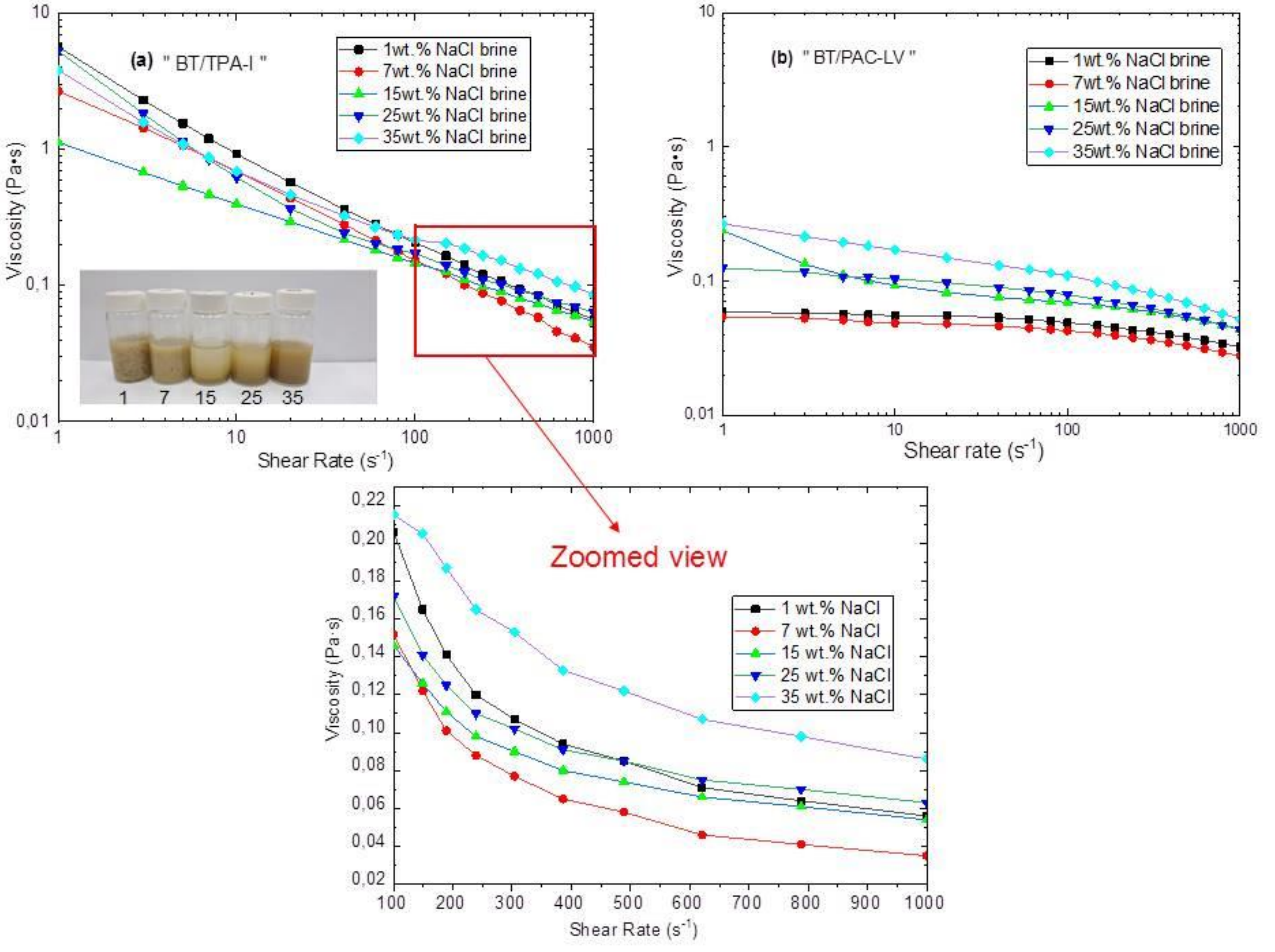

Fig. 11 Steady shear viscosity of 2% BT/TPA-I (a) and BT/PAC-LV (b) polymer dispersions over a wide range of shear rates and NaCl concentrations at 25 °C.

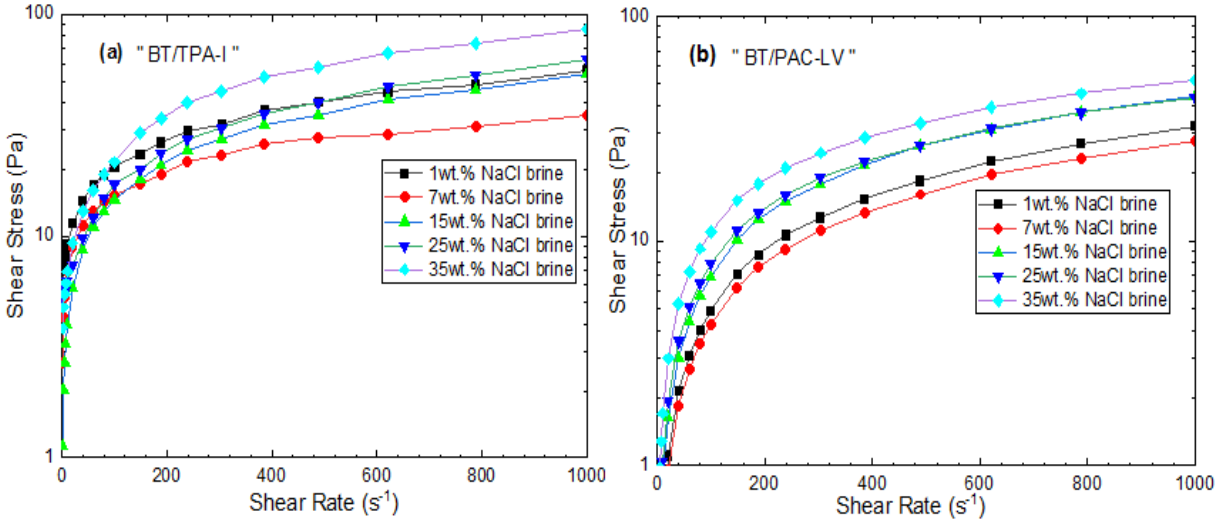

Fig. 12 Flow curves of the BT/TPA-I (a) and BT/PAC-LV (b) polymer dispersions across a wide range of shear rate and NaCl concentrations at 25 °C.

Table 3. Parameters of Herschel-Bulkley model for bentonite/terpolymer dispersions prepared in different brines at 25 °C.

Concentration of brine, wt.%		1	7	15	25	35
BT with TPA-I	YS (pa)	4.08	1.68	1.13	5.29	2.99
	K (pa•s^n)	1.54	1.06	0.54	1.14	1.1
	n	0.31	0.54	0.11	0.23	0.22
	GS 10s (Pa)	18.8	1.14	3.54	10.7	20.5
	GS 10min (Pa)	25.8	1.1	3.68	11.1	21
BT with PAC-LV	YS (pa)	-0.12	-0.07	0.15	0.08	0.24
	K (pa•s^n)	0.05	0.05	0.11	0.11	0.19
	n	0.01	0.01	0.02	0.02	0.04
	GS 10s (Pa)	0.41	0.18	0.54	0.054	0.81
	GS 10min (Pa)	0.36	0.21	0.39	0.47	0.75

*YS - yield stress, K - consistency coefficient, n - flow behavior index, GS - gel strength.

A high YS value is an important factor for the application of drilling fluid in drilling well operations as it facilitates the easy transport of shale cuttings to the surface of the hole and improves the efficiency of cleaning the drilling well.

With regards to the K, in the case with BT/TPA-I the increase of salinity from 1 to 15 wt.% NaCl resulted in the decrease of K from 1.54 Pa·s^n to 0.54 Pa·s^n. However, the further increase of salinity up to 35 wt.% NaCl resulted in the increase of K to the value of 1.1 Pa·s^n. Of note, in the case with BT/PAC-LV the value of K did not exceed 0.19 Pa·s^n over a wide range of NaCl concentrations.

The value of the n is determined by evaluating the slope of a logarithmic plot depicting the relationship between shear stress and shear rate. A value of n greater than 1 indicates that the fluid exhibits shear-thickening characteristics, whereas a value of n less than 1 signifies shear-thinning behavior. It is worth emphasizing that the effective viscosity of a non-Newtonian fluid is influenced not only by rheological parameters but also by the local shear rate, which is significantly impacted by the movement of particles in a two-phase flow. When n is less than 1, the fluid is categorized as pseudo-plastic, which is commonly observed in solutions of polymers or suspensions containing fine solid particles.[14] Indeed, the value of the n indicates that all BT/TPA-I formulations exhibit shear-thinning (pseudo-plastic) behavior within the salinity range of 1-35 wt.% NaCl. This confirms that the bentonite/terpolymer composites display shear-thinning behavior at high concentrations of NaCl. These rheological properties make the TPA suitable for use in combination with bentonite as a rheology modifier in brine salt-resistant WBDF. The ability to control the rheological behavior of drilling fluids is crucial for efficient drilling operations, and the incorporation of TPA can contribute to achieving the desired flow characteristics under high salinity conditions.

Demonstrates the GS of BT/TPA-I and BT/PAC-LV formulations prepared in 1, 7, 15, 25 and 35 wt.% brines, respectively (See Fig. 13).

As Fig. 13(a) shows, both 10-seconds and 10-minutes GS values decrease with the increase of salinity from 1 to 15 wt.% NaCl. However, the further increase of salinity to 35 wt.% NaCl results in the increase of the GS values. Of note is that BT/TPA-I formulation failed to provide a GS value required by the API standard only in 15 wt.% NaCl brine. Whereas for

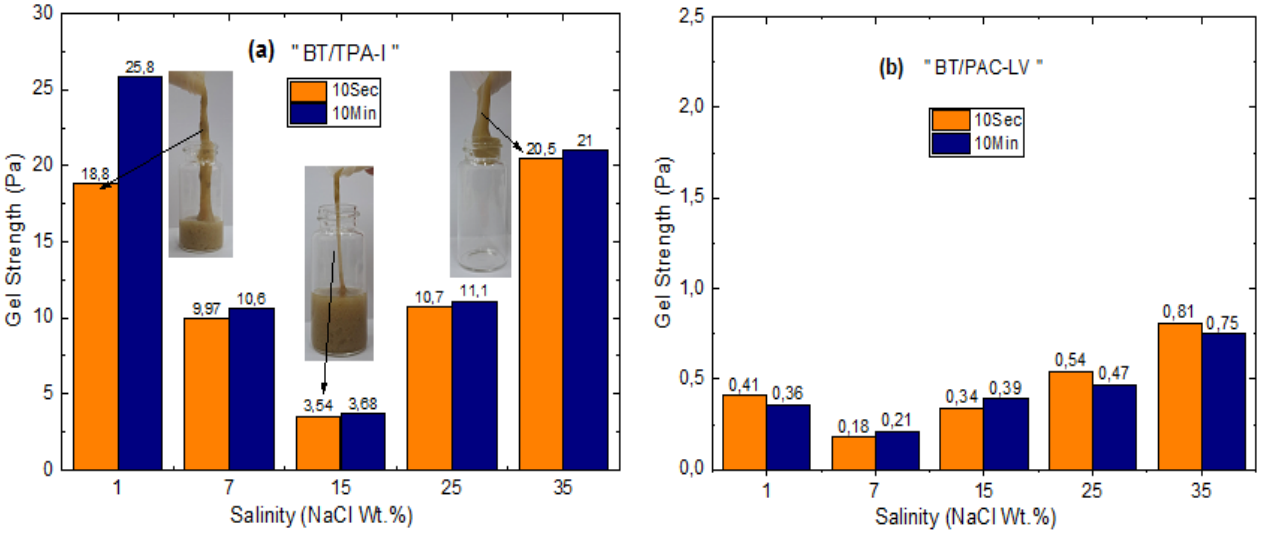

Fig. 13 GS of BT/TPA-I (a) and BT/PAC-LV (b) dispersions within a wide range of NaCl concentration at 25 °C.

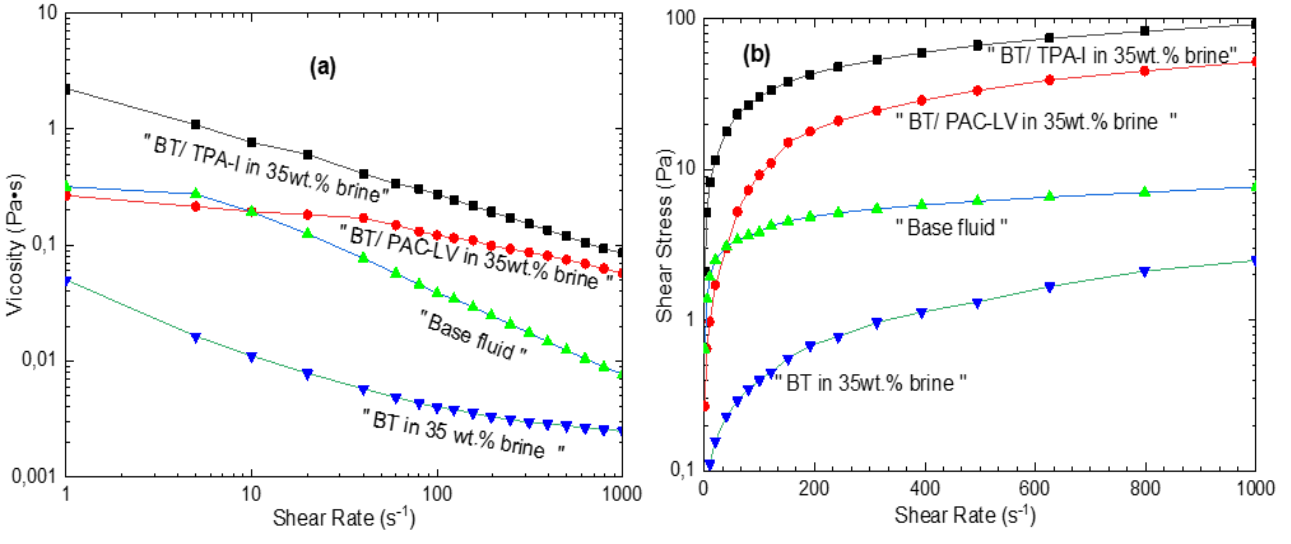

Fig. 14 Viscosity (a) and flow curves (b) of different drilling fluid formulations prepared in 35 wt.% NaCl brine at 25°C.

other concentrations of NaCl the GS values were notably higher than the numbers required by the standard. At the same time BT/PAC-LV could not provide the required GS values in the same conditions (see Fig. 13(b)). This proves the effectiveness of BT/TPA-I over BT/PAC-LV.

3.5.4 Comparative rheological behavior of different drilling fluids at a high salinity of brine

Figure 14(a) demonstrates the viscosity versus shear rate for bentonite suspensions prepared in distilled water and 35 wt.% NaCl brine. As can be seen, bentonite suspension in distilled water possesses sufficiently higher viscosity values within the range of shear rates from 1 to 1000 s^{-1}. This can be explained by the swelling of bentonite in distilled water. However, in high salinity brines the effect of swelling the clay particles is less pronounced due to the presence of ions. The introduction of PAC-LV resulted in the increase of viscosity at 5 s^{-1} from 0.0164 to 0.215 Pa·s. However, the introduction of TPA-I resulted in the increase of viscosity to 1.09 Pa·s in the same conditions. Of note is that at 1000 s^{-1} the viscosity of BT/TPA-I was 1.5 times higher than that of BT/PAC-LV.

Base fluid and BT/TPA-I in 35 wt.% NaCl dispersions exhibited the highest YS values of 0.64 and 2.99 Pa, respectively (Fig. 14b). This information is presented in Table 4.

Table 4. Rheological parameters of Herschel-Bulkley model for different formulations of bentonite and bentonite/polymers.

Drilling fluid formulations	YS(Pa)	K(Pa·s^n)	n
Base fluid	0.64	0.27	0.05
BT+35wt.% brine	0.05	0.01	0.02
BT/PAC-LV+35 wt.% brine	0.24	0.12	0.04
BT/TPA-I+35 wt.% brine	2.99	1.1	0.22

As Table 4 shows, the lowest YS (0.05 Pa) and K (0.01 Pa·s^n) were observed for bentonite suspension prepared by using 35 wt.% NaCl brine. Whereas the highest YS (2.99 Pa) and K (1,1 Pa·s^n) were observed for BT/TPA-I formulation in

35 wt.% NaCl brine.

3.6 Fluid loss tests

In all filtration tests the resulting filtrate appeared colorless, indicating that it mainly consisted of water. However, the initial attempt to perform the fluid-loss filtration test using BT+35 wt.% NaCl brine was unsuccessful. The filter cake formation was inadequate, leading to the complete loss of water from the bentonite/brine dispersion. This failure could be attributed to the presence of a channel at the center of the filter cake.

Figure 15 illustrates the fluid-loss versus time for different formulations. The findings reveal a notably higher initial filtration rate in the first 5 minutes, which can be attributed to the absence of a filter cake structure at the beginning of the filtration process. Following this, the filtration rate progressively decreases in 5-minute intervals, indicating the gradual formation of the filter cake. Among the different formulations, the Base fluid dispersion demonstrates the highest fluid loss. This discovery suggests that the addition of polymers to the bentonite dispersion enhances filtration performance and mitigates the extent of fluid loss.

In the fluid loss tests with Base fluid, the filter cake exhibited small pores and channels, which allowed for increased water flow and resulted in a high volume of filtrate. However, upon the addition of polymers to the bentonite dispersions, the filtration rate and total fluid loss noticeably decreased. This reduction in fluid loss can be attributed to the adsorption of polymer molecules onto the bentonite platelets. The presence of long linear chain molecules in the terpolymer prevents water penetration through the filter cake and forms a stable, thin layer that blocks the filter cake pores. This is showed in Fig. 16. The filtration performance of the bentonite and bentonite/polymer dispersions exhibited a distinct trend in terms of fluid-loss values. Specifically, for a filtration duration of 30 minutes, the observed trend was the following: BT/TPA-I < BT/PAC-LV < Base Fluid.

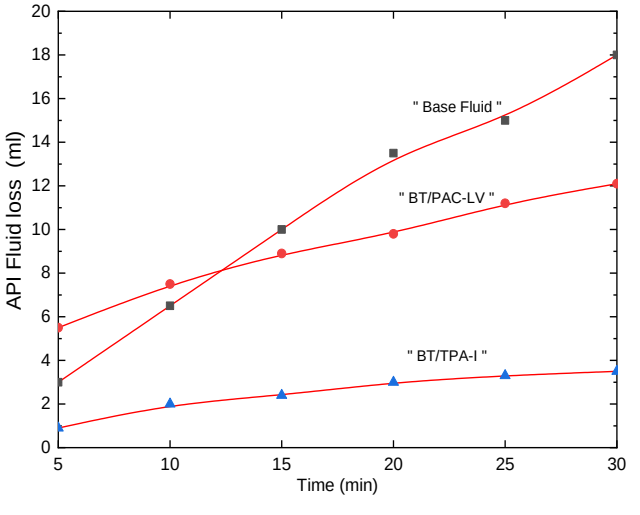

Fig. 15 Fluid loss volume vs time for Base fluid, BT/TPA and BT/PAC-LV drilling fluid formulations in 35 wt.% NaCl at 25 °C.

The BT/TPA-I formulation with high salinity exhibited a significantly lower fluid-loss volume, measuring only 3.5 mL, which is well below the API standard limit of 12 mL. Furthermore, the filter cake thickness was measured at 0.09 cm, and the permeability of the filter cake was determined to be 1.17 mD. The thinness and low permeability of the filter cake contributed to the minimal volume of fluid loss.

The results suggest that the TPA-I terpolymer shows promising potential in reducing fluid loss in water-based drilling fluids (WBDF) when operating under high salinity conditions and at room temperature.

3.6.1 Permeability of filter cake, and SEM analysis

The permeability of the filter cake was calculated from Darcy's law[14]:

$$dV_f/dt = k \cdot A \cdot \Delta P/\mu h_c \quad (3)$$

where,
filtrate volume (V_f) in cubic centimeters;
filtration time (t) in seconds;
pressure drop across the filter cake (ΔP) in kPa;
area of the filter cake medium (A) in cm^2;
viscosity of the filtrate (μ) in Pa·s;
thickness of the filter cake (h_c) in cm;
and permeability of the filter cake (k) typically expressed in microdarcies (μD).

When measuring the permeability of the filter cake, it is assumed that three parameters remain constant: the pressure drop across the filter cake (690 kPa), the area of the filter medium (22.3 cm^2), and the viscosity of the filtrate (8.90×10^{-4} Pa·s).

Table 5 presents the permeability of the filter cakes after fluid-loss filtration. Among the tested formulations, the BT/35 wt.% brine dispersion exhibited the highest permeability value (26.7 mD), along with a filter cake thickness of 0.41 cm. In comparison, the addition of PAC-LV and TPA-I polymers to the BT dispersion resulted in a significant reduction in permeability to 7.9 and 1.17 mD, respectively, accompanied by a decrease in filter cake thickness to 0.18 and 0.09 cm, respectively.

Specifically, PAC-LV dispersion shows a 3.3 times reduction in permeability, while the BT/TPA-I dispersion exhibits a substantial 22.8 times reduction in permeability. In addition to its lower permeability, the BT/TPA-I dispersion exhibits the minimum filter cake thickness compared to all other BT and BT/polymer dispersions. This minimal filter cake thickness offers several advantages. Firstly, it restricts the invasion of the fluid loss volume into the wellbore formations, minimizing potential damage. Secondly, the reduced filter cake thickness facilitates smoother drilling operations and mitigates the risk of differential pipe sticking issues.

Four SEM images of the filter cakes were taken to examine the impact of bentonite and terpolymers on their surface morphology. Among all the filter cake SEM analyses, the filter cake produced by the BT/TPA-I dispersion exhibited the most compact structure compared to the filter cakes of other BT and

BT/polymer dispersions.

The images represented in Figs. 16(a) and 16(b) display the filter cake formed by BT dispersions, exhibiting an open structure characterized by numerous micro cracks, scattered arrangements, and nanopores. The presence of these nanopores contributes to the highest levels of permeability and thickness observed in the filter cake of BT dispersions. However, when TPA-I terpolymer is incorporated into the BT dispersions containing high salinity, notable improvements in the texture of the filter cakes are observed.

The reduced permeability of the BT/polymer dispersion filter cakes can be attributed to the bridging mechanism between BT micro-particles and nanoscale polymer chains. The bridging between BT platelets and polymer chains leads to the formation of a multilayer thin structure in the filter cake, resulting in a more compact and compressed structure. Upon evaluating all the filter cakes, it becomes apparent that the filter cake derived from the BT/TPA-I dispersion, as shown in Fig. 15(c), exhibits a highly compact structure with the lowest permeability and thickness compared to the filter cakes of other formulations (Table 5).

It is important to note that the filter cake obtained from the BT/TPA-I dispersion outperforms the BT/PAC-LV filter cake. The BT/TPA-I filter cake is characterized by a homogeneous nanostructure, suggesting a more uniform and compact arrangement.

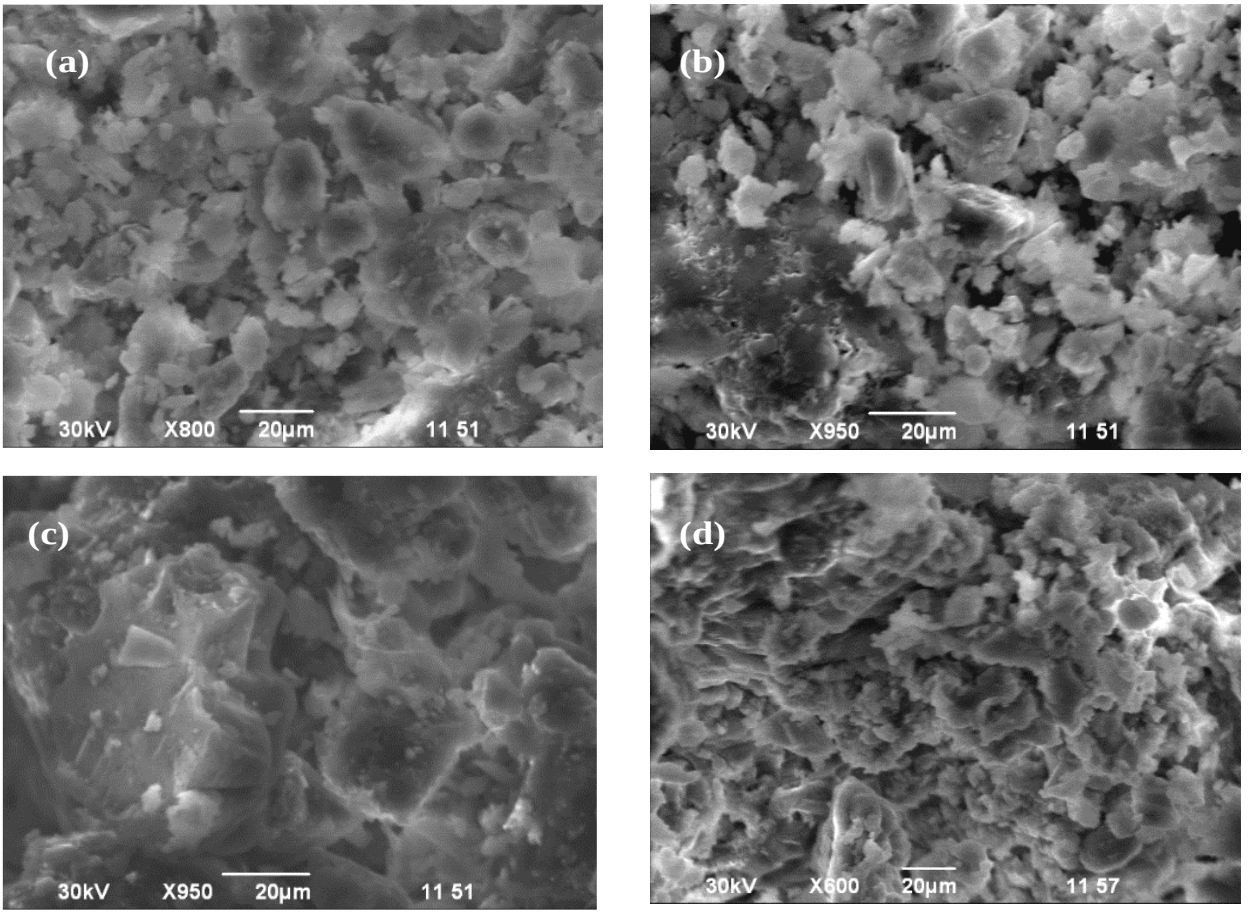

Fig. 16 SEM images of bentonite/polymer-based mud cakes after fluid-loss filtration tests at 25 °C; (a) sample 4% BT in deionized water (without polymer); (b) sample 4% BT + 35% NaCl brine (without polymer); (c) sample 4% BT + 2% TPA-I + 35% NaCl brine; (d) sample 4% BT+2% PAC-LV+ 35% NaCl brine.

Table 5. Fluid loss, thickness and permeability of filter cakes after fluid-loss filtration tests.

Drilling fluid formulations	Filtrate volume V_f (cm^3)	Filter cake Thickness h_c (cm)	Permeability of filter cakes k (mD)	Ratio of permeability to thickness k/h_c (mD/cm)
Base fluid	18	0.35	15.3	43.71
BT+35% brine	totally loss	0.41	26.7	65.12
BT/PAC-LV+35% brine	12.1	0.18	7.9	43.89
BT/TPA-I+35% brine	3.5	0.09	1.17	13

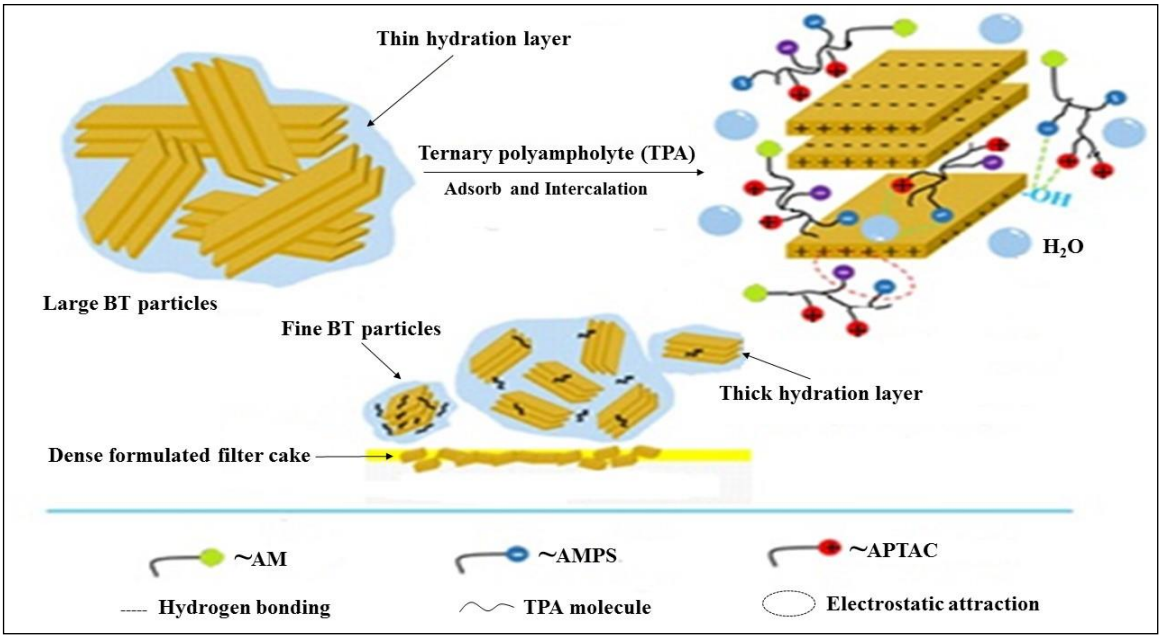

Fig. 17 Schematic representation of interaction between bentonite platelets and TPA chains.

4. On the mechanism of stabilization drilling fluids

Earlier[39,40] we have shown that the charged-balanced polyampholyte based on amphoteric terpolymer AAm-*co*-AMPS-*co*-APTAC (80:10:10 mol.%) exhibits excellent salt tolerance in high saline synthetic brine (containing NaCl, KCl, $MgCl_2$, and $CaCl_2$ salts) in the range of salt concentrations from 250 to 300 $g.L^{-1}$. Such behavior of TPA was explained by so called antipolyelectrolyte effect as a result of screening the positively and negatively charged monomers by added salts leading to expansion (or unfolding) the macromolecular chains. Therefore, for the TPA an increase in solution viscosity and a significant enhancement in rheological properties in high salinity brine is observed. Authors [31,33-35] also developed highly salt-resistant drilling fluids based on various polyampholytes with bentonite and cationic copolyelectrolyte additives on drilling fluids for shales[41,42] In our case application of the TPA-I noticeably enhanced the rheological properties of bentonite/polymer dispersions, such as apparent viscosity, YS, and GS, even in 35 wt.% NaCl brine at 25 °C. As a result, it was considered a suitable choice for drilling fluid applications. The excellent rheological properties of the BT/TPA-I dispersion can be attributed to the strong chemical interactions between the functional groups of the terpolymer and the positively charged edges of the bentonite platelets. The interaction between bentonite and TPA in brine can be explained by two distinct mechanisms. The first mechanism is adsorption of terpolymer onto bentonite. The second mechanism is ionic interaction between the negatively charged functional groups of macromolecules and the positively charged edges of bentonite platelets[14] (Fig. 17).

5. Conclusions

Ternary polyampholyte (TPA) based on AAm-*co*-AMPS-*co*-APTAC terpolymer was synthesized and tested as an additive to the WBDFs compared to standard fluid loss additive – PAC-LV. The intrinsic viscosity of TPA in 35 wt.% of NaCl solution is 10 times higher than that of PAC-LV. The dynamic viscosity of 2 wt.% TPA solution at high shear rate (1000 s^{-1}) increases from 34 to 90 mPa·s with increase in brine salinity from 1 to 35 wt.% adjusted by NaCl while the dynamic viscosity of PAC-LV increased from 27 to 46 mPa·s with increase of NaCl concentration from 1 to 35 wt.%. The values of GS of BT/TPA drilling fluid after 10 s and 10 min were equal to 20.5 and 21 Pa, respectively. The same parameters for BT/PAC-LV cellulose drilling fluid were equal to 0.81 and 0.75 Pa, respectively after 10 s and 10 min. Moreover, all BT/TPA-I formulations exhibit shear-thinning (pseudo-plastic) behavior within the salinity range of 1-35 wt.% NaCl. It should be noted that the GS of BT/TPA drilling fluid decreases with increase the salinity from 1 to 15 wt.% while the further increase the salinity up to 35 wt.% resulted in the increase of GS. Among all tested formulations, the BT/TPA drilling fluid exhibited the lowest filtrate volume, filter cake thickness, and permeability under high brine salinity conditions. SEM images demonstrate that the filter cake obtained by using BT/TPA drilling fluid is characterized by the most compact arrangement of particles. The superior effectiveness of BT/TPA drilling fluid compared to BF, BT/brine water, or BT/PAC-LV drilling fluids at high salinity brines is due to antipolyelectrolyte effect, *e.g.* the unfolding of macromolecular chains leading to increase the viscosity. This confirms that the BT/TPA drilling fluids exhibit remarkable shear-thinning behavior at high concentrations of NaCl. Such rheological properties make the amphoteric terpolymer AAm-*co*-AMPS-*co*-APTAC as suitable rheology enhancer in high salinity brine for salt-resistant WBDF in combination with bentonite. Controlling the rheological behavior of drilling fluids is crucial for efficient drilling operations, and the inclusion of amphoteric terpolymer can

contribute to achieving the desired flow characteristics under high shear rate and salinity conditions at 25 °C.

Acknowledgements

This research was funded by the Science Committee of the Ministry of Science and Higher Education of the Republic of Kazakhstan under Grant № AP14972771. Authors thank Prof. Nurxat Nuraje at Nazarbayev University for provision of assistance in providing of ^{1}H-NMR, ^{13}C-NMR, TEM and elemental analysis.

References

[1] Z. Luo, J. Pei, L. Wang, P. Yu, Z. Chen, Influence of an ionic liquid on rheological and filtration properties of water-based drilling fluids at high temperatures, *Applied Clay Science*, 2017, **136**, 96-102, doi: 10.1016/j.clay.2016.11.015.

[2] N. Wahid, M. A. Yusof, N. H. Hanafi, Optimum Nanosilica Concentration in Synthetic Based Mud (SBM) for High Temperature High Pressure Well, *SPE/IATMI Asia Pacific Oil & Gas Conference and Exhibition. OnePetro*, 2015, doi: 10.2118/176036-ms.

[3] V. Mahto, V. P. Sharma, Rheological study of a water based oil well drilling fluid, *Journal of Petroleum Science and Engineering*, 2004, **45**, 123-128, doi: 10.1016/j.petrol.2004.03.008.

[4] L.-M. Zhang, Y.-B. Tan, Z.-M. Li, Application of a new family of amphoteric cellulose-based graft copolymers as drilling-mud additives, *Colloid and Polymer Science*, 1999, **277**, 1001-1004, doi: 10.1007/s003960050482.

[5] A. Aftab, A. R. Ismail, Z. H. Ibupoto, H. Akeiber, M. G. K. Malghani, Nanoparticles based drilling muds a solution to drill elevated temperature wells: a review, *Renewable and Sustainable Energy Reviews*, 2017, **76**, 1301-1313, doi: 10.1016/j.rser.2017.03.050.

[6] G. T. Teixeira, R. F. Lomba, S. A. Fontoura, V. A. Melendez, E. C. Ribeiro, A. D. Francisco, R. S. Nascimento, New material for wellbore strengthening and fluid losses mitigation in deepwater drilling scenario, *SPE Deepwater Drilling and Completions Conference. SPE*, 2014, doi:10.2118/170266-ms.

[7] M.-C. Li, Q. Wu, K. Song, S. Lee, C. Jin, S. Ren, T. Lei, Soy protein isolate As fluid loss additive in bentonite-water-based drilling fluids, *ACS Applied Materials & Interfaces*, 2015, **7**, 24799-24809, doi: 10.1021/acsami.5b07883.

[8] W. Shan, J. Ma, G. Jiang, J. Sun, Y. An. An inverse emulsion polymer as a highly effective salt- and calcium-resistant fluid loss reducer in water-based drilling fluids, *ACS Omega*, 2022, **7**, 16141-16151, doi: 10.1021/acsomega.2c01476.

[9] Z. -Q. Xiong, X. -D. Li, F. Fu, Y. N. Li, Performance evaluation of laponite as a mud-making material for drilling fluids, *Petroleum Science*, 2019, **16**, 890-900, doi: 10.1007/s12182-018-0298-y.

[10] K. Y. Choo, K. Bai, Effects of bentonite concentration and solution pH on the rheological properties and long-term stabilities of bentonite suspensions, *Applied Clay Science*, 2015, **108**, 182-190, doi: 10.1016/j.clay.2015.02.023.

[11] L. Hammadi, N. Boudjenane, M. Belhadri, Effect of polyethylene oxide (PEO) and shear rate on rheological properties of bentonite clay, *Applied Clay Science*, 2014, **99**, 306-311, doi: 10.1016/j.clay.2014.07.016.

[12] K, B. Azouz, Influence of the temperature on the rheological properties of bentonite suspensions in aqueous polymer solutions, *Applied Clay Science*, 2016, **123**, 92-98, doi: 10.1016/j.clay.2016.01.016.

[13] B. Abu-Jdayil, M. Ghannam, M. S. Nasser, The modification of rheological properties of bentonite-water dispersions with cationic and anionic surfactants, *International Journal of Chemical Engineering and Applications*, 2016, **7**, 75-80, doi: 10.7763/ijcea.2016.v7.546.

[14] H. Mudaser, Ahmad, High molecular weight copolymers as rheology modifier and fluid loss additive for water-based drilling fluids, *Journal of Molecular Liquids*, 2018, **252**, 133-143, doi: 10.1016/j.molliq.2017.12.135.

[15] K. Abdiyev, M. Marić, B. Orynbaev, M. Zhursumbaeva, N. Seitkaliyeva, Z. Toktarbay, A novel cationic polymer surfactant for regulation of the rheological and biocidal properties of the water-based drilling muds, *Polymers*, 2023, **15**, 330, doi: 10.3390/polym15020330.

[16] J. Sun, C. Deng, X. Chen, H. Yu, H. Tian, J. Sun, X. Jing, Self-assembly of polypeptide-containing ABC-type triblock copolymers in aqueous solution and its pH dependence, *Biomacromolecules*, 2007, **8**, 1013-1017, doi: 10.1021/bm0609792.

[17] Y.-J. Che, Y. Tan, J. Cao, H. Xin, G.-Y. Xu, Synthesis and properties of hydrophobically modified acrylamide-based polysulfobetaines, *Polymer Bulletin*, 2011, **66**, 17-35, doi: 10.1007/s00289-010-0255-4.

[18] H. Mao, W. Wang, Y. Ma, Y. Huang, Synthesis, characterization and properties of an anionic polymer for water-based drilling fluid as an anti-high temperature and anti-salt contamination fluid loss control additive, *Polymer Bulletin*, 2021, **78**, 2483-2503, doi: 10.1007/s00289-020-03227-y.

[19] H. Jamshidi, A. Rabiee, Synthesis and characterization of acrylamide-based anionic copolymer and investigation of solution properties, *Advances in Materials Science and Engineering*, 2014, **2014**, 1-6, doi: 10.1155/2014/728675.

[20] S. Davoodi, A. Ramazani S A, A. Soleimanian, A. Fellah Jahromi, Application of a novel acrylamide copolymer containing highly hydrophobic comonomer as filtration control and rheology modifier additive in water-based drilling mud, *Journal of Petroleum Science and Engineering*, 2019, **180**, 747-755, doi: 10.1016/j.petrol.2019.04.069.

[21] M. Amanullah, M. K. AlArfaj, Z. Al-abdullatif, Preliminary Test Results of Nano-based Drilling Fluids for Oil and Gas Field Application, *SPE/IADC drilling conference and exhibition. SPE*, 2011, doi:10.2118/139534-ms.

[22] S. Sepehri, R. Soleyman, A. Varamesh, M. Valizadeh, A. Nasiri, Effect of synthetic water-soluble polymers on the properties of the heavy water-based drilling fluid at high pressure-high temperature (HPHT) conditions, *Journal of Petroleum Science and Engineering*, 2018, **166**, 850-856, doi:

10.1016/j.petrol.2018.03.055.
[23] J. Fink, Petroleum Engineer's Guide to Oil Field Chemicals and Fluids, *Gulf Professional Publishing*, 2012, doi: 10.1016/C2009-0-61871-7.
[24] N. Mohamadian, H. Ghorbani, D. A. Wood, M. A. Khoshmardan, A hybrid nanocomposite of poly(styrene-methyl methacrylate- acrylic acid)/clay as a novel rheology-improvement additive for drilling fluids, *Journal of Polymer Research*, 2019, **26**, 1-14, doi: 10.1007/s10965-019-1696-6.
[25] M.-C. Li, Q. Wu, K. Song, Y. Qing, Y. Wu, Cellulose nanoparticles as modifiers for rheology and fluid loss in bentonite water-based fluids, *ACS Applied Materials & Interfaces*, 2015, **7**, 5006-5016, doi: 10.1021/acsami.5b00498.
[26] F. T. G. Dias, R. R. Souza, E. F. Lucas, Influence of modified starches composition on their performance as fluid loss additives in invert-emulsion drilling fluids, *Fuel*, 2015, **140**, 711-716, doi: 10.1016/j.fuel.2014.09.074.
[27] M. Amanullah, L. Yu, Environment friendly fluid loss additives to protect the marine environment from the detrimental effect of mud additives, *Journal of Petroleum Science and Engineering*, 2005, **48**, 199-208, doi: 10.1016/j.petrol.2005.06.013.
[28] M.-C. Li, Q. Wu, K. Song, C. F. De Hoop, S. Lee, Y. Qing, Y. Wu, Cellulose nanocrystals and polyanionic cellulose as additives in bentonite water-based drilling fluids: rheological modeling and filtration mechanisms, *Industrial & Engineering Chemistry Research*, 2016, **55**, 133-143, doi: 10.1021/acs.iecr.5b03510.
[29] F. Liu, G. Jiang, S. Peng, Y. He, J. Wang, Amphoteric polymer as an anti-calcium contamination fluid-loss additive in water-based drilling fluids, *Energy & Fuels*, 2016, **30**, 7221-7228, doi: 10.1021/acs.energyfuels.6b01567.
[30] G. S. Georgiev, E. B. Kamenska, E. D. Vassileva, I. P. Kamenova, V. T. Georgieva, S. B. Iliev, I. A. Ivanov, Self-assembly, antipolyelectrolyte effect, and nonbiofouling properties of polyzwitterions, *Biomacromolecules*, 2006, **7**, 1329-1334, doi: 10.1021/bm050938q.
[31] A. Rabiee, A. Ershad-Langroudi, H. Jamshidi, Polyacrylamide-based polyampholytes and their applications, *Reviews in Chemical Engineering*, 2014, **30**, 501-519, doi: 10.1515/revce-2014-0004.
[32] B. A. Hamad, M. He, M. Xu, W. Liu, M. Mpelwa, S. Tang, L. Jin, J. Song, A novel amphoteric polymer as a rheology enhancer and fluid-loss control agent for water-based drilling muds at elevated temperatures, *ACS Omega*, 2020, **5**, 8483-8495, doi: 10.1021/acsomega.9b03774.
[33] F. Liu, G. Jiang, S. Peng, Y. He, J. Wang, Amphoteric polymer as an anti-calcium contamination fluid-loss additive in water-based drilling fluids, *Energy & Fuels*, 2016, **30**, 7221-7228, doi: 10.1021/acs.energyfuels.6b01567.
[34] F. Wang, J. Yang, J. Zhao, Understanding anti-polyelectrolyte behavior of a well-defined polyzwitterion at the single-chain level, *Polymer International*, 2015, **64**, 999-1005, doi: 10.1002/pi.4907.
[35] J. Li, J. Sun, K. Lv, Y. Ji, J. Liu, X. Huang, Y. Bai, J. Wang, J. Jin, S. Shi, Temperature- and salt-resistant micro-crosslinked polyampholyte gel as fluid-loss additive for water-based drilling fluids, *Gels*, 2022, **8**, 289, doi: 10.3390/gels8050289.
[36] Yang, L., Xie, C., Ao, T., Cui, K., Jiang, G., Bai, B., & Tian, W, Comprehensive evaluation of self-healing polyampholyte gel particles for the severe leakoff control of drilling fluids, *Journal of Petroleum Science and Engineering*, 2022, **212**, 110249, doi: 10.1016/j.petrol.2022.110249.
[37] A. Vipulanandan, A. Mohammed, Effect of drilling mud bentonite contents on the fluid loss and filter cake formation on a field clay soil formation compared to the API fluid loss method and characterized using Vipulanandan models, *Journal of Petroleum Science and Engineering*, 2020, **189**, 107029, doi: 10.1016/j.petrol.2020.107029.
[38] S. Bagherian, Aghdam, Synthesis and performance evaluation of a novel polymeric fluid loss controller in water-based drilling fluids: high-temperature and high-salinity conditions, *Journal of Natural Gas Science and Engineering*, 2020, **83**, 103576, doi: 10.1016/j.jngse.2020.103576.
[39] I. Gussenov, N. Mukhametgazy, A. Shakhvorostov, S. Kudaibergenov, Synthesis and characterization of high molecular weight amphoteric terpolymer based on acrylamide, 2-acrylamido-2-methyl-1-propanesulfonic acid sodium salt and (3-acrylamidopropyl)trimethylammonium chloride for oil recovery, *Chemical Bulletin of Kazakh National University*, 2021, **103**, 12-20, doi: 10.15328/cb1243.
[40] I. S. Gussenov, N. Mukhametgazy, A. V. Shakhvorostov, S. E. Kudaibergenov, Comparative study of oil recovery using amphoteric terpolymer and hydrolyzed polyacrylamide, *Polymers*, 2022, **14**, 3095, doi:10.3390/polym14153095.
[41] M. Beg, P. Singh, S. Sharma, U. Ojha, Shale inhibition by low-molecular-weight cationic polymer in water-based mud, *Journal of Petroleum Exploration and Production Technology*, 2018, **9**, 1995-2007, doi: 10.1007/s13202-018-0592-7.
[42] M. Beg, S. Sharma, U. Ojha, Effect of cationic copolyelectrolyte additives on drilling fluids for shales, *Journal of Petroleum Science and Engineering*, 2017, **12**, 009, doi: 10.1016/j.petrol.2017.